Lab on a Chip

Drawing Sensors on Chips: Deposition of Carbon-Based Materials on Diverse Surfaces by Mechanical Abrasion

Journal:	*Lab on a Chip*
Manuscript ID:	LC-ART-07-2014-000864
Article Type:	Paper
Date Submitted by the Author:	24-Jul-2014
Complete List of Authors:	Frazier, Kelvin; Massachsetts Institute of Technology, Chemistry Mirica, Katherine; Massachsetts Institute of Technology, Chemistry Walish, Joseph; Massachsetts Institute of Technology, Chemistry Swager, Timothy; Massachusetts Institute of Technology, Department of Chemistry

Lab on a Chip

RSCPublishing

PAPER

Fully-Drawn Carbon-Based Chemical Sensors on Organic and Inorganic Surfaces

Cite this: DOI: 10.1039/x0xx00000x

Kelvin M. Frazier, Katherine A. Mirica, Joseph J. Walish and Timothy M. Swager*

Received 00th January 2012,
Accepted 00th January 2012

DOI: 10.1039/x0xx00000x

www.rsc.org/

Mechanical abrasion is an extremely simple, rapid, and low cost method for deposition of carbon-based materials onto a substrate. However, the method is limited in throughput, precision, and surface compatibility for drawing conductive pathways. Selective patterning of surfaces using laser etching can facilitate substantial improvements to address these current limitations for the abrasive deposition of carbon-based materials. This study demonstrates the successful on-demand fabrication of fully-drawn chemical sensors on a wide variety of substrates (e.g., weighing paper, polymethyl methacrylate, silicon, and adhesive tape) using single-walled carbon nanotubes (SWCNTs) as sensing materials and graphite as electrodes. Mechanical mixing of SWCNTs with solid or liquid selectors yields sensors that can detect and discriminate parts-per-million (ppm) quantities of various nitrogen-containing vapors (pyridine, aniline, triethylamine).

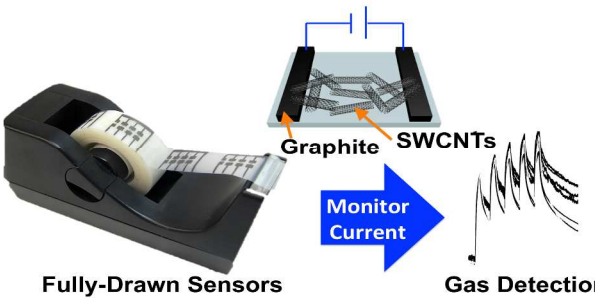

Introduction

Chemical sensors that identify and monitor volatile organic compounds (VOCs) have an important role in assessing public security, food and water quality, industrial environment, and health.[1–7] For example, it would be useful to detect residual volatile organic compounds (VOCs) in consumer goods such as food,[8,9] shelter,[9,10] clothing,[11] and medicine[9] and to protect workers from occupational exposure. Presently, the monitoring and determination of the chemical components of gas samples is typically done using gas chromatography-mass spectrometry (GC-MS).[10–13] This technique, although highly sensitive and selective, has the disadvantages of limited portability, high cost, and requirement of highly trained users.

Carbon nanotubes (CNTs), are useful materials in chemical sensing as a result of the sensitivity of their electrical conductance to the presence of chemical analytes.[3,5,14] A productive route to enhancing the selectivity and sensitivity of these materials to specific analytes is covalent or non-covalent functionalization with polymers, metals, or small molecules.[15–25] Straightforward integration of these materials into devices on various substrates can yield simple, portable, and low-power sensors and arrays capable of detecting and differentiating a wide variety of vapors at parts-per-million (ppm) concentrations.[16,17,19,20,22,23,26–32]

The fabrication of sensing devices by printing[33–38], dip coating[36,38,39], drop casting[40], photolithography[41], or drawing[34–39,42–44] has advantages of being simple and low-cost without the need for highly specialized facilities. Drawing is particularly attractive because it directly deposits carbon-based solid composite materials that require no solution-phase processing.[33,34,36,38,42,43] Recently, we[42,43] and others[33,34,38] have developed methods for the fabrication of carbon-based sensors on the surface of paper by drawing. Taken together, these methods are capable of producing functional chemiresistors[34,38,42,43], electrochemical sensors[36,38], strain and pressure sensors[34], and simple electrodes[35,36,38,39,44] from commercially available starting materials within minutes. Although the abrasive deposition of solid sensing materials on the surface of cellulose paper has made the fabrication of chemical sensors from carbon nanomaterials simple, solvent-free, and easily accessible, there are limitations to this method. The location, size, thickness, and distribution of the resulting conductive carbon "film"

Lab on a Chip RSCPublishing

PAPER

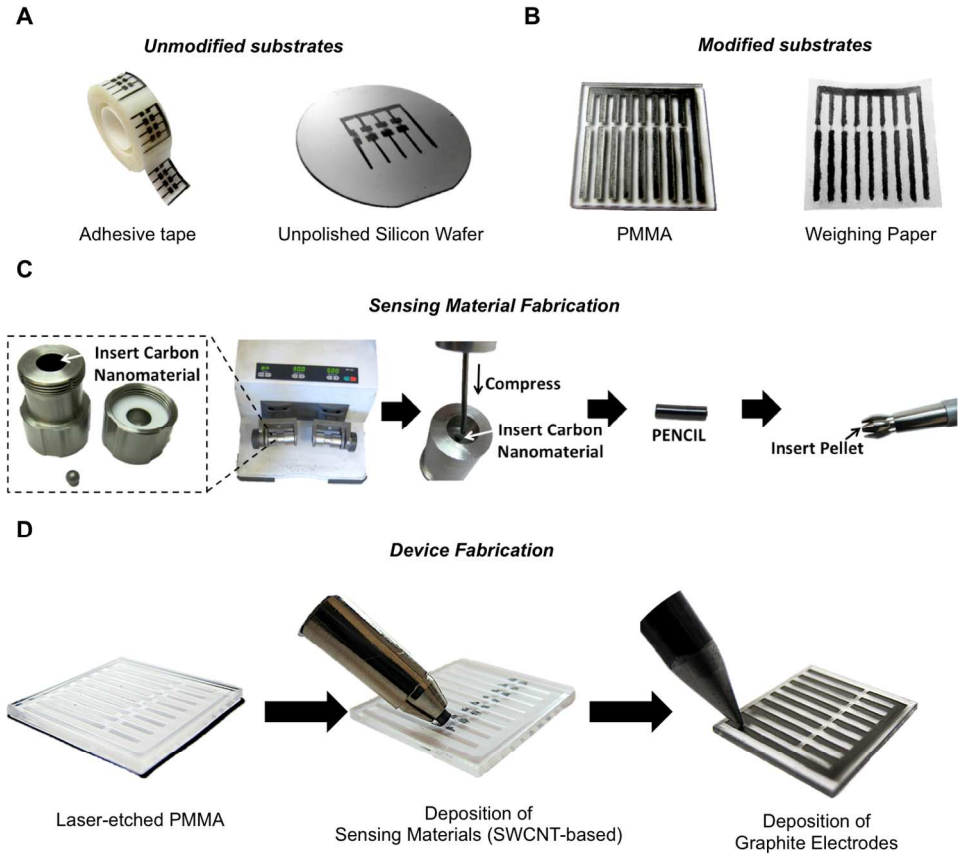

Fig 1. Fabrication of chemiresistive chemical sensors by drawing. Sensing materials (SWCNT-based) and graphite as electrodes were both deposited by mechanical abrasion to yield fully-drawn, chemiresistive gas-sensors on various A) unmodified substrates such as adhesive tape and unpolished silicon wafer, and B) laser-etched substrates such as PMMA and weighing paper. C) Fabrication of the sensing material consists of mechanically mixing and compressing SWCNT composites into a pellet. D) Stepwise fabrication of fully drawn chemiresistive sensors on PMMA.

is difficult to control and limited by the features of the substrate (e.g., surface roughness and distribution of cellulose fibers on the surface of paper).

Herein we describe a rapid, scalable, portable, and cost-effective approach for the on-demand fabrication of fully-drawn chemical sensing arrays on a variety of different substrates (e.g., paper, plastic, and undoped silicon wafer). This approach is entirely solvent-free, requires only small amounts of sensory materials, and is capable of producing highly-sensitive chemical sensors. We demonstrate this approach in the context of sensing and differentiating a variety of nitrogen-containing vapors at ppm concentrations. Our demonstration employs solid composites of single-walled carbon nanotubes (SWCNTs) with small molecules as the sensing material and graphite as electrodes. We utilize a previously established method[43] to generate sensing materials, or PENCILs (**P**rocess **E**nhanced **N**ano**C**arbon for **I**ntegrated **L**ogic), by the mechanical mixing of SWCNTs with commercially available small molecules (solid or liquid). We then utilize DRAFT (**D**eposition of **R**esistors with **A**brasion **F**abrication **T**echnique) to deposit these materials on a variety of substrates. Sequential deposition by mechanical abrasion of sensing materials and commercial graphite pencils on selected etched (weighing paper and PMMA) and non-etched (silicon wafer and adhesive tape) substrates yields precisely fabricated fully-drawn chemiresistive sensing arrays (**Figure 1**).

Results and Discussion

Partially-Drawn Sensors: Mechanical Abrasion of Only Chemiresistive Materials. The successful stepwise fabrication of fully-drawn chemiresistive sensors consist of two separate deposition steps: deposition of sensing materials (SWCNTs) and deposition of electrodes (graphite). In order to measure the performance of each deposition step separately, we fabricated partially-drawn sensors where we evaluated compatibility of various substrates with DRAFT, and then selected four substrates to

demonstrate the performance and versatility of the fully-drawn sensors.

Partially-drawn sensors were made by depositing sensing materials by mechanical abrasion (SWCNT:Selector) between and on top of gold electrodes on six different substrates: weighing paper, glass, silicon, alumina, polymethyl methacrylate (PMMA), and adhesive tape. To evaluate the sensory performance of each device, we used pyridine (an industrial hazard[9]) as a model analyte. To increase the response of the SWCNTs to pyridine vapor we chose to make SWCNT composites with triethyl citrate (TEC), which is a commercial, nontoxic, colorless, and odorless liquid used as a food additive and plasticizer.[45] Mechanical mixing and compression of SWCNTs with TEC can coat and disperse SWCNTs within a solid composite of a PENCIL and enable hydrogen-bonding interactions between the hydroxyl groups of TEC and the lone pair of pyridine, thus enhancing the sensitivity of the SWCNT/TEC composite towards pyridine. These PENCILs are stable under ambient conditions and can be used to produce devices over the course of at least two months without any decrease in sensory performance (**Figure S7**).

To establish compatibility of substrates with DRAFT we fabricated devices by abrading a composite of SWCNTs and TEC (2:1 wt. ratio) onto six different substrates equipped with gold electrodes (1 mm gap size). The resulting devices generated significant changes in conductance when exposed to 50 ppm pyridine vapour under a constant bias (50 mV). **Figure 2A** displays normalized conductance traces of devices exposed five consecutive times to 50 ppm pyridine for 30 s with 60 s recovery time on six different substrates. The functionalized CNT chemiresistors have a semi-reversible response towards pyridine for all devices. The first exposure provided the largest response consistently. By exempting the first exposure we lower the coefficients-of-variance of our sensors in response to 50 ppm pyridine between 2-16% (**Table S1**).

To investigate the dynamic sensing range of the substrates, devices were exposed to various concentrations of pyridine (1-550 ppm) for five consecutive cycles of 30 s exposures with 60 s recovery times (**Figure 2B & 2C**). The first exposure to pyridine was excluded from the device's average normalized conductance response as a result of its irreversibility and large variability (~10% coefficient-of-variance at 50 ppm pyridine on weighing paper). The sensors from each substrate can successfully detect pyridine at its permissible exposure limit (1ppm: American Conference of Governmental Industrial Hygienists [ACGIH]) and discriminate it from higher values (e.g., 20 ppm) (**Figure S16**). Five of the six substrates examined demonstrated a similar magnitude (at 50 ppm pyridine: $\Delta G/G_0$= 5.2-8.3%) of the conductive response towards pyridine. The sixth substrate, glass, was characterized by the poorest sensing performance (at least 2 times lower) across the range of concentrations examined.

We used profilometry to investigate the surface morphology of the six substrates. From these data we were able to calculate the root-mean-square (RMS) surface roughness of weighing paper (RMS = 2.5 ± 0.7 μm), alumina (RMS = 1.1 ± 0.3 μm), adhesive tape (RMS = 1.7± 0.7 μm), unpolished side of the undoped silicon wafer (RMS = 1.2 ± 0.1 μm), PMMA (RMS = 0.05 ± 0.02 μm), and glass (RMS = 5.9 ± 0.5 nm). The abrasion of the TEC/SWCNT PENCIL on glass was both challenging and produced non-uniform and poorly distributed films of nanotubes as a result of the hardness and smoothness of the substrate. In order to facilitate the deposition of PENCILs by abrasion on smooth surfaces, we modified substrates (PMMA and glass) by laser or chemical etching. However, the laser-etched glass did not facilitate improved deposition of materials by DRAFT as a result of surface artifacts and cracks on the surface of the glass that we introduced by the etching process (**Figure S4**).

Graphite Electrodes by Mechanical Abrasion. After investigating DRAFT on various substrates, we endeavoured to produce electrodes by abrasion to yield a fully-drawn CNT-based

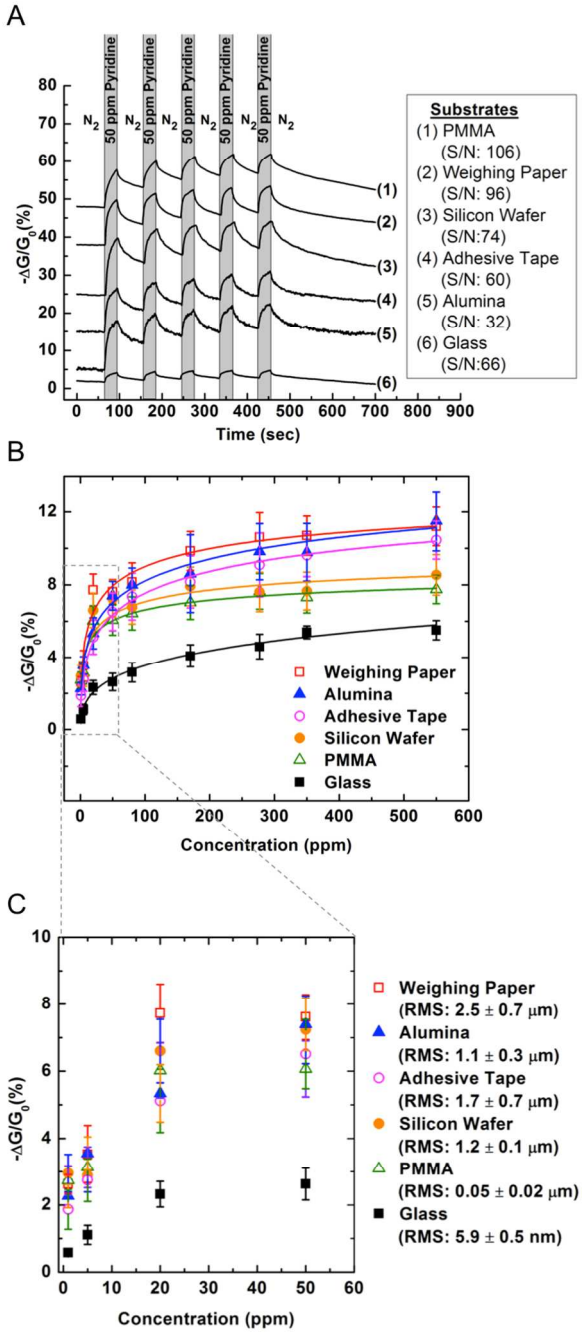

Fig 2. Mechanical deposition of sensing materials on six different substrates. A) Comparison of changes in conductance of sensing materials deposited on six different substrates in response to five consecutive exposures to 50 ppm pyridine. B-C) The average normalized conductance response (first exposure exempt) of at least six sensors on each substrate upon five consecutive exposures to various concentrations of pyridine for 30 s with 60 s recovery time.

Lab on a Chip RSCPublishing

PAPER

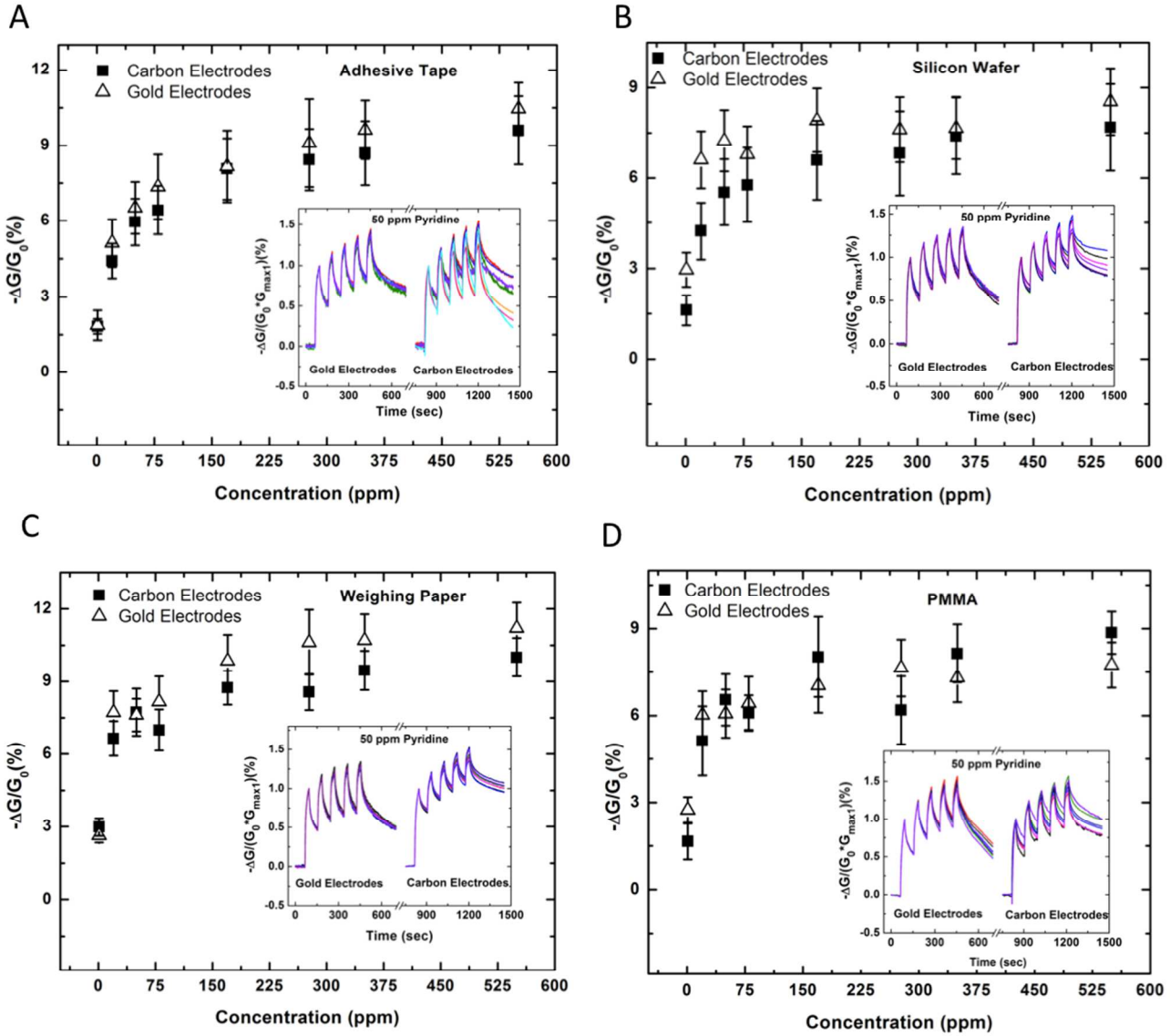

Fig 3. Comparison of device performance between fully-drawn sensors (SWCNT:TEC (1:2 wt. ratio) deposited by DRAFT and carbon-based electrodes deposited by mechanical abrasion) verses partially-drawn sensors (SWCNT:TEC (1:2 wt. ratio) deposited by DRAFT and gold electrodes deposited by thermal evaporation). A-D) Average normalized conductive response (first exposure exempt) of at least four fully-drawn sensors (black squares) and partially drawn sensors (white triangles) simultaneously exposed to various concentrations of pyridine for 30 s with 60 s recovery time. Inset: Normalized conductance over time of seven fully-drawn and seven partially-drawn devices.

chemiresistive array. To facilitate the successful design of a fully-drawn chemiresistor, it is imperative that the electrodes of the sensor are substantially more conductive and largely inert to the chemical analytes. To explore this requirement, we compared the response of pristine SWCNTs to the response of a commercial 9B graphite pencil when both were abraded between gold electrodes on the surface of weighing paper (3 sensors each) and exposed to various analytes. The resistive range of the sensors was 1-2 kΩ. The sensing response of graphite was 5 times smaller in response to 277 ppm pyridine than the response of pristine SWCNTs (**Figure S12**). This study suggests that SWCNTs are much more sensitive materials than graphite towards a wide range of chemical analytes, a difference that should be amplified even further when the sheet resistance of graphite electrodes within a chemiresistor architecture is substantially lower than that of SWCNT-based sensing materials.

Fabrication of Fully-Drawn Chemical Sensors. Fully-drawn sensors have the advantage of being easily fabricated on-demand or

replaced. We demonstrate the fabrication and characterize sensing performance of fully-drawn chemical sensors on four different substrates (**Figure 3**). We implement a two-step fabrication process to generate fully-drawn working devices (**Figure 3A-B**) on the unmodified surface of adhesive tape and an unpolished undoped highly resistive (resistance >10000 Ω-cm) silicon wafer. The first step involves drawing a line of sensing material (SWCNT:TEC) approximately 3 mm in length having a resistance of 400-600 kΩ. The second step then generates carbon-based electrodes by abrasion of a graphite pencil on top of the sensing material leaving a 1 mm gap between the electrodes. A stainless steel mask was used as a stencil to guide the deposition of graphite-based electrodes and to protect 1 mm of the CNT-based sensing material from contamination by graphite.

This two-step fabrication method is however limited to surfaces that facilitate efficient abrasion of graphite pencils to generate conductive electrodes (conductive line of 2.2 cm must have a resistance values < 9 kΩ). Graphite does not abrade efficiently on smooth surfaces (e.g., weighing paper and PMMA) and yields electrodes with unacceptably high sheet resistance (**Figure S13**). This limitation can be overcome by introducing an additional step into the fabrication procedure by increasing surface roughness of the substrate through chemical or laser etching. This additional step has an added advantage of localizing the abrasion of graphite into pre-defined regions on the chip. Using this strategy, we demonstrate the ability to precisely fabricate fully-drawn working devices on laser-etched surfaces of weighing paper and PMMA (**Figure 3C-D**). We believe that this method is transferable to many substrates.

Comparing Performance of Fully-Drawn and Partially-Drawn Sensors. **Figure 3** successfully demonstrates that the average normalized conductive response of the resulting chemiresistors with carbon-based electrodes is comparable to the standard gold electrode upon exposures to several concentrations of pyridine on various substrates. The plot (**Figure 3**) displays the average normalized conductive responses (first exposure exempt) of at least four devices with either gold electrodes or carbon-based electrodes simultaneously exposed five consecutive times to various concentrations of pyridine for 30 s with 60 s recovery times. The inset displays the normalized conductance trace (additionally normalized to the first exposure) over time of seven devices with either gold electrodes or carbon-based electrodes simultaneously exposed five consecutive times to 50 ppm pyridine for 30 s with 60 s recovery time. Device-to-device variation was investigated between fully-drawn and partially-drawn sensors on 4 substrates (weighing paper, PMMA, silicon, and adhesive tape) using SWCNT:TEC as sensing material and graphite or gold as electrodes. At least 7 devices were exposed 5 consecutive times to 50 ppm pyridine 30 s with 60 s recovery times. The fully-drawn sensors yields slightly higher (1-5%) coefficient-of-variance in response to pyridine compared to the partially drawn sensors (weighing paper: fully-drawn sensor [12%] and partially-drawn sensor [9%]) excluding the first exposure to pyridine (**Table S1 & S4**).

Fully-Drawn Sensing Arrays. The fabrication of fully-drawn chemical sensors is a general concept that can be extended to chemical sensing arrays. To illustrate this concept, we generated different sensing materials by mechanical mixing of SWCNTs with a solid selector, two different ionic liquids, or a plasticizer to draw a SWCNT-based chemiresistive array (**Figure 4**). The chemical structures of the selectors used are shown in **Figure 4A**. Selector **1L** was discussed earlier for pyridine sensing. Selector **2L** and **3L** are ionic liquids that have been previously used in conjunction with graphene and a quartz crystal microbalance to detect benzene.[46] Selector **1S** is a solid selector with a functional group handle (hexafluoroisopropanol) that has been previously used to detect Dimethyl methylphosphonate (DMMP) vapor via hydrogen-bond acids.[47–50] These selector:SWCNT composites were abrasion deposited over an etched pattern on the weighing paper. Graphite was then abraded on top of the etched pattern on the weighing paper leaving gap size of 1 mm between the electrodes. The chemiresistive array was then exposed to a variety of gas analytes that can be classified as biomarkers[12,51], nerve agents[23,50], industrial hazards[9], quality of food markers[9,51,52], and gasoline.[13] To investigate the selectivity of the devices that were fully-drawn and placed into array, we exposed the devices five consecutive times to various analytes for 30 s with a 60 s recovery time. The color scale mapping of

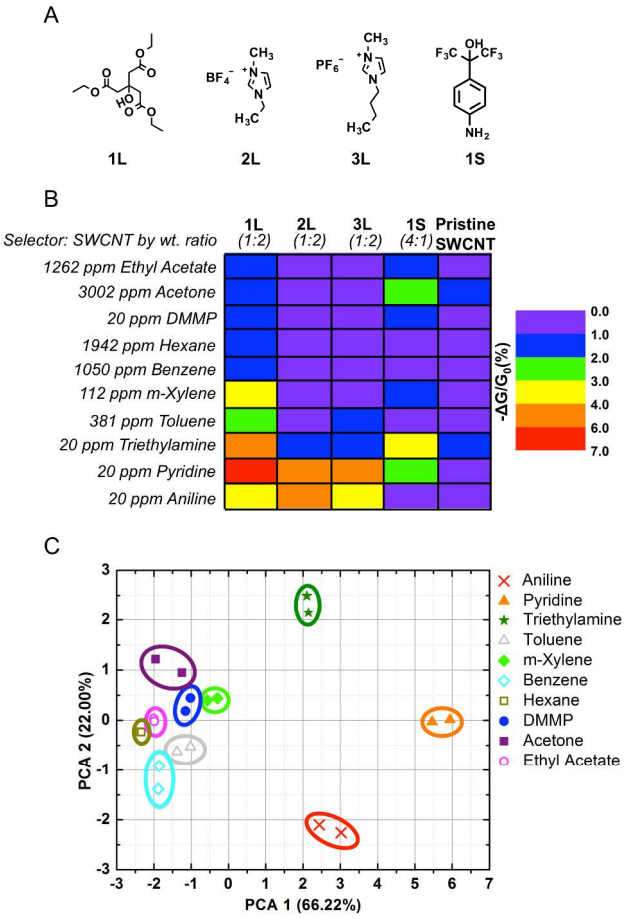

Fig 4. Fully-Drawn Sensor Array. A) Schematic diagram of the selector's chemical structure used in the sensor array. L represents selectors that are liquids (Bp > 200°C) and S represents selectors that are solids at room temperature prior to mixing with SWCNTs. The selectors were mixed with pristine SWCNTs mechanically and compressed into a pellet to make PENCILs. B) Average normalized conductive response (first exposure exempt) to simultaneous exposure to various gas analytes at ppm concentrations 5 consecutive times for 30 s with a 60 s recovery time. The PENCILs were deposited by DRAFT on weighing paper and the carbon-based electrodes (with 1 mm gap size) were deposited by abrasion using graphite pencil on the etched surface of weighing paper. C) Principal Component Analysis (PCA) plot discriminates between various gas analytes from the average conductive responses (first exposure exempt) of the sensor array.

the average normalized change of conductance (first exposure exempt) of fully-drawn devices is presented in **Figure 4B**. Each selector had enhancements in sensitivity and selectivity towards certain analytes compared to pristine SWCNTs. As predicted, selector **1S** caused the SWCNTs to be more sensitive towards DMMP, however the enhancement was modest (1.3 times higher sensitivity). We speculate that in this formulation the hexafluoroisopropanol group is engaged in intermolecular hydrogen bonding with the aniline moiety thereby reducing the binding of DMMP. The ionic liquid selectors **2L** and **3L** did not show enhancements towards benzene possibly due to the change in morphology from graphene (flat) to carbon nanotubes (cylindrical) or change in sensing method from monitoring mass change (quartz crystal microbalance) to current change (chemiresistor). However, **2L** and **3L** did provide high selectivity towards amines and low sensitivity towards other analytes. The lone pair of electrons from the amines can interact with the ionic liquid to possibly cause charge separation thus enhancing the SWCNTs sensitivity and selectivity. Selector **1L** displayed the highest sensitivity towards pyridine. The average normalized conductive response (first exposure exempted) of the fully-drawn CNT-based chemiresistive array towards various analytes was analyzed using Principle Component Analysis (PCA) (**Figure 4C**). The four-component array can successfully discriminate nitrogen-containing compounds from one another (pyridine, aniline, and triethylamine) and from other VOCs at low ppm concentration levels. Aniline and triethylamine are additional amines that are of interest since aniline has been reported as a possible biomarker for patients with lung cancer and triethylamine has been reported as a possible biomarker for patients with renal failure.[51] This array lays the groundwork for detecting and differentiating amines of interest in occupational safety.

Conclusion

Abrasion over pre-patterned substrates successfully expands the scope of DRAFT in throughput, precision, and surface compatibility. Etching substrates (e.g., laser or chemical) enhanced the ability to control the location and other structural aspects of conductive carbon structures deposited on a variety of surfaces using DRAFT. This general strategy enabled the fabrication of fully-drawn chemiresistors on weighing paper, PMMA, adhesive tape, and an undoped silicon wafer by mechanical abrasion. Fully-drawn arrays on weighing paper were capable of detecting and discriminating low ppm concentrations of N-containing vapors (pyridine, aniline, and triethylamine). This fabrication methodology does not require specialized facilities (e.g., clean room, thermal evaporator) and can be performed entirely on a desktop (with appropriate ventilation and safety precautions for handling nanomaterials). The method lays the groundwork for expanding the capabilities of the fabrication of functional sensors, circuits, and tags by drawing on a variety of surfaces. This method can also be used towards a more efficient and rapid parallel fabrication of multiple devices by abrading surfaces of carbon materials against pre-pattered substrates. We believe this type of strategy can facilitate controlled deposition of sensing materials and electrodes onto pre-defined regions on various surfaces.

Experimental Section

Fabrication of PENCILs. Triethyl Citrate (Cat. No. 109290) and 1-Ethyl-3-methylimidazolium tetrafluoroborate (Cat. No. 39736) were purchased from Sigma Aldrich. 2-(4-Aminophenyl)-1,1,1,3,3,3-hexafluoro-2-propanol (Cat. No. B24048) and 1-n-Butyl-3-methylimidazolium hexafluorophosphate (Cat. No. L19086) were purchased from Alfa Aesar. Purified SWCNTs (> 95 % SWCNTs) were provided by Nano-C, Inc (Westwood, MA). All chemicals and reagents were used without further purification, unless noted otherwise. SWCNTs, selector, and 7 mm diameter stainless steel grinding balls were added into a 5 ml stainless steel ball milling vial. The vial was placed into a mixing mill (MM400, Retsch GmbH, Haan, Germany) where the carbon material was mechanically mixed at 30 Hz for 5 min under ambient conditions. The SWCNTs:selector mixture was then placed into a custom-made stainless steel pellet mold with 2 mm internal diameter where the SWCNT composites were compressed (Carver Press, Model # 3912) for 1 min to make PENCILs.

Fabrication of Partially-Drawn Sensors. Glass slides (Cat. No. 16004-422, VWR International) were cleaned by ultra-sonication in acetone for 30 min and dried using a stream of nitrogen. The glass slides were then cleaned with an UV Ozone Cleaner (Model No. 2, Jelight Company, Irvine, CA, http://www.jelight.com) for 10 min. PMMA (Cat. No. 8560K172, 1/16" thick, McMaster-Carr) substrates were cleaned by ultra-sonication in soapy water for 15 min followed by sonication in methanol for another 15 min and dried using a stream of nitrogen. Alumina (Cat. No. 8462K21, 0.025" thick, McMaster-Carr) substrates were cleaned by ultra-sonication for 15 min in soapy water and another 15 min in acetone and dried using a stream of nitrogen. Silicon wafer (Cat. No. SIUc50D05C1-HHR, MTI Corporation), weighing paper (Cat. No. 12578-165, VWR International), and adhesive tape (Item 487908, Model 52380P12, Invisible tape, Staples) was used without any further modification.

Using a stainless steel mask (purchased from Stencils Unlimited, Lake Oswego, OR, http://www.stencilsunlimited.com), layers of chromium (10 nm) and gold (75 nm) were deposited onto the substrate using thermal evaporation (Angstrom Engineering, Kitchener, Ontario, Canada). There was a 1 mm gap between the metal electrodes. The PENCILs were inserted into a holder (Item No. DA, Alvin Tech DA) and deposited using DRAFT between and on top of the metal electrodes until 100-500 kΩ resistance range was achieved on each substrate (as measured across the electrode gap with a multimeter); except for unpolished side of the silicon wafer, where 6-8 kΩ resistance range was achieved.

Laser-Etching Procedure. A Universal Laser Systems model VLS4.60 equipped with a 60 Watt laser was used for all laser-etching operations. The power, speed, and pulses-per-inch settings were adjusted to provide suitable etching on each substrate type. A listing of exact parameters can be found in the supplemental information (**Table S2**).

Fabrication of Fully-Drawn Sensors. The substrates were cleaned as stated previously. PENCILs were inserted into a holder (Alvin Tech DA) and deposited by DRAFT onto a substrate to generate a conductive line approximately 3 mm in length until 400-600 kΩ resistance range was achieved. Carbon-based electrodes with 1 mm gap size were deposited on top of the SWCNTs composites by abrasion using a graphite pencil (Faber-Castell PITT Graphite Pure Woodless 2900 9B) purchased from Artist and Craftsmen (Cambridge, MA). A stainless steel mask protected approximately 1 mm of the sensing material from contamination by graphite. The graphitic layers were deposited until a certain range of sheet resistance was obtained (**Table S3**).

Investigation of the Sensory Performance of Devices. The sensor chip was placed in a 2 × 30 pin edge connector and enclosed in a home-made Teflon enclosure equipped with an inlet, an outlet, and an internal channel for gas flow. Measurements of current were

performed under a constant applied voltage of 50 mV using a PalmSense EmStat-MUX equipped with a 16-channel multiplexer (Palm Instruments BV, The Netherlands). The current through the sensor was monitored while exposing it to various analytes (delivered using Kin-Tech gas generator: Precision Gas Standards Generator Model 491M-B, La Marque, TX) with dry nitrogen as the carrier gas five consecutive times for 30 s with a recovery time of 60 s.

Acknowledgements

This work was funded by the Army Research Office through the Institute for Soldier Nanotechnologies, the Defence Advanced Projects Agency, and the National Institutes of Health under Ruth L. Kirschstein National Research Service Award F32CA157197 from the National Cancer Institute (KAM). We thank Nano-C, Inc. for kindly providing purified SWCNTs for this study.

Notes and references

Department of Chemistry, Massachusetts Institute of Technology, 77 Massachusetts Avenue, Cambridge, MA 02139 United States. Tel: +1 (617) 253 4423 Email: tswager@mit.edu

† Electronic Supplementary Information (ESI) available. See DOI: 10.1039/b000000x/

1. J. A. Griffith and T. S. Bayer, *Sens. Actuators B Chem.*, 2014, **190**, 818–821.
2. J. Zhou, K. Xu, P. Zhou, O. Zheng, Z. Lin, L. Guo, B. Qiu, and G. Chen, *Biosens. Bioelectron.*, 2014, **51**, 386–390.
3. J. Kong, N. R. Franklin, C. Zhou, M. G. Chapline, S. Peng, K. Cho, and H. Dai, *Science*, 2000, **287**, 622–625.
4. K. J. Albert, N. S. Lewis, C. L. Schauer, G. A. Sotzing, S. E. Stitzel, T. P. Vaid, and D. R. Walt, *Chem. Rev.*, 2000, **100**, 2595–2626.
5. Y. Liu, X. Dong, and P. Chen, *Chem. Soc. Rev.*, 2012, **41**, 2283–2307.
6. M.-I. Mohammed and M. P. Y. Desmulliez, *Lab. Chip*, 2011, **11**, 569–595.
7. C. Escobedo, *Lab. Chip*, 2013, **13**, 2445–2463.
8. J. W. Gardner, T. C. Pearce, S. Friel, P. N. Bartlett, and N. Blair, *Sens. Actuators B Chem.*, 1994, **18**, 240–243.
9. C. Elosua, C. Bariain, I. R. Matias, A. Rodriguez, E. Colacio, A. Salinas-Castillo, A. Segura-Carretero, and A. Fernandez-Gutiérrez, *Sensors*, 2008, **8**, 847–859.
10. H. Wang, L. Nie, J. Li, Y. Wang, G. Wang, J. Wang, and Z. Hao, *Chin. Sci. Bull.*, 2013, **58**, 724–730.
11. J. S. Schreiber, S. House, E. Prohonic, G. Smead, C. Hudson, M. Styk, and J. Lauber, *Risk Anal.*, 1993, **13**, 335–344.
12. L. Dong, X. Shen, and C. Deng, *Anal. Chim. Acta*, 2006, **569**, 91–96.
13. L.-W. Jia, M.-Q. Shen, J. Wang, and M.-Q. Lin, *J. Hazard. Mater.*, 2005, **123**, 29–34.
14. J. Y. Kim, J. Lee, S. Hong, and T. D. Chung, *Chem. Commun.*, 2011, **47**, 2892–2894.
15. S. Daniel, T. P. Rao, K. S. Rao, S. U. Rani, G. R. K. Naidu, H.-Y. Lee, and T. Kawai, *Sens. Actuators B Chem.*, 2007, **122**, 672–682.
16. J. M. Schnorr and T. M. Swager, *Chem. Mater.*, 2011, **23**, 646–657.
17. K. Balasubramanian and M. Burghard, *Small*, 2005, **1**, 180–192.
18. C. Dyke and J. Tour, in *Carbon Nanotubes*, CRC Press, 2006, pp. 275–294.
19. K. M. Frazier and T. M. Swager, *Anal. Chem.*, 2013, **85**, 7154–7158.
20. J. Kong, M. G. Chapline, and H. Dai, *Adv. Mater.*, 2001, **13**, 1384–1386.
21. R. J. Chen, Y. Zhang, D. Wang, and H. Dai, *J. Am. Chem. Soc.*, 2001, **123**, 3838–3839.
22. F. Wang and T. M. Swager, *J. Am. Chem. Soc.*, 2011, **133**, 11181–11193.
23. F. Wang, H. Gu, and T. M. Swager, *J. Am. Chem. Soc.*, 2008, **130**, 5392–5393.
24. L. Hu, D. S. Hecht, and G. Grüner, *Chem. Rev.*, 2010, **110**, 5790–5844.
25. J. M. Lobez, S.-J. Han, A. Afzali, and J. B. Hannon, *ACS Nano*, 2014.
26. J. M. Schnorr, D. van der Zwaag, J. J. Walish, Y. Weizmann, and T. M. Swager, *Adv. Funct. Mater.*, 2013, **23**, 5285–5291.
27. J. Li, Y. Lu, Q. Ye, M. Cinke, J. Han, and M. Meyyappan, *Nano Lett.*, 2003, **3**, 929–933.
28. Q. Cao and J. A. Rogers, *Adv. Mater.*, 2009, **21**, 29–53.
29. P. Qi, O. Vermesh, M. Grecu, A. Javey, Q. Wang, H. Dai, S. Peng, and K. J. Cho, *Nano Lett.*, 2003, **3**, 347–351.
30. D. R. Kauffman and A. Star, *Angew. Chem. Int. Ed.*, 2008, **47**, 6550–6570.
31. K. G. Ong, K. Zeng, and C. A. Grimes, *IEEE Sens. J.*, 2002, **2**, 82–88.
32. P. Bondavalli, P. Legagneux, and D. Pribat, *Sens. Actuators B Chem.*, 2009, **140**, 304–318.
33. N. Dossi, R. Toniolo, A. Pizzariello, F. Impellizzieri, E. Piccin, and G. Bontempelli, *ELECTROPHORESIS*, 2013, **34**, 2085–2091.
34. C.-W. Lin, Z. Zhao, J. Kim, and J. Huang, *Sci. Rep.*, 2014, **4**.
35. K. ul Hasan, O. Nur, and M. Willander, *Appl. Phys. Lett.*, 2012, **100**, 211104.
36. E. W. Nery and L. T. Kubota, *Anal. Bioanal. Chem.*, 2013, **405**, 7573–7595.
37. N. Kurra, D. Dutta, and G. U. Kulkarni, *Phys. Chem. Chem. Phys.*, 2013, **15**, 8367–8372.
38. N. Kurra and G. U. Kulkarni, *Lab. Chip*, 2013, **13**, 2866–2873.
39. A. J. Gimenez, J. M. Yáñez-Limón, and J. M. Seminario, *J. Phys. Chem. C*, 2011, **115**, 282–287.
40. G. Aragay, H. Montón, J. Pons, M. Font-Bardía, and A. Merkoçi, *J. Mater. Chem.*, 2012, **22**, 5978–5983.
41. A. W. Martinez, S. T. Phillips, Z. Nie, C.-M. Cheng, E. Carrilho, B. J. Wiley, and G. M. Whitesides, *Lab. Chip*, 2010, **10**, 2499–2504.
42. K. A. Mirica, J. G. Weis, J. M. Schnorr, B. Esser, and T. M. Swager, *Angew. Chem.*, 2012, **51**, 10740–10745.
43. K. A. Mirica, J. M. Azzarelli, J. G. Weis, J. M. Schnorr, and T. M. Swager, *Proc. Natl. Acad. Sci.*, 2013, E3265–E3270.
44. B. Yao, L. Yuan, X. Xiao, J. Zhang, Y. Qi, J. Zhou, J. Zhou, B. Hu, and W. Chen, *Nano Energy*, 2013, **2**, 1071–1078.
45. H.-M. Park, M. Misra, L. T. Drzal, and A. K. Mohanty, *Biomacromolecules*, 2004, **5**, 2281–2288.
46. Q. Ji, I. Honma, S.-M. Paek, M. Akada, J. P. Hill, A. Vinu, and K. Ariga, *Angew. Chem.*, 2010, **122**, 9931–9933.
47. L. S. Fifield and J. W. Grate, *Carbon*, 2010, **48**, 2085–2088.
48. P. Xu, X. Li, H. Yu, M. Liu, and J. Li, *J. Micromechanics Microengineering*, 2010, **20**, 115003.
49. Y. Yang, Y. Chen, P. Xu, and X. Li, *Microelectron. Eng.*, 2010, **87**, 2317–2322.

50. H. Li, Q. Zheng, J. Luo, Z. Cheng, and J. Xu, *Sens. Actuators B Chem.*, 2013, **187**, 604–610.
51. B.-P. Jiang, D.-S. Guo, and Y. Liu, *J. Org. Chem.*, 2011, **76**, 6101–6107.
52. N. Funazaki, A. Hemmi, S. Ito, Y. Asano, Y. Yano, N. Miura, and N. Yamazoe, *Sens. Actuators B Chem.*, 1995, **25**, 797–800.